LA-UR-12-24334
Approved for public release; distribution is unlimited.

Title: Irradiation Embritlement in Alloy HT-Â-9

Author(s): Serrano De Caro, Magdalena

Intended for: Report

Irradiation Embritlement in Alloy HT-9

M. Caro
Los Alamos National Laboratory

July 17, 2012

Table of Contents

Summary

HT-9 steel is a candidate structural and cladding material for high temperature lead-bismuth cooled fast reactors. In typical advanced fast reactor designs fuel elements will be irradiated for an extended period of time, reaching up to 5-7 years. Significant displacement damage accumulation in the steel is expected (> 200 dpa) when exposed to dpa-rates of 20-30 dpa_{Fe}/y and high fast flux (E > 0.1 MeV) ~4 x 10^{15} n/cm^2s. Core temperatures could reach 400-560°C, with coolant temperatures at the inlet as low as 250°C, depending on the reactor design [1,2]. Mechanical behavior in the presence of an intense fast flux and high dose is a concern. In particular, low temperature operation could be limited by irradiation embrittlement. Creep and corrosion effects in liquid metal coolants could set a limit to the upper operating temperature.

In this report, we focus on the low temperature operating window limit and describe HT-9 embrittlement experimental findings reported in the literature that could provide supporting information to facilitate the consideration of a Code Case on irradiation effects for this class of steels in fast reactor environments. HT-9 has an extensive database available on irradiation performance, which makes it the best choice as a possible near-term candidate for clad, and ducts in future fast reactors. Still, as it is shown in this report, embrittlement data for very low irradiation temperatures (< 200°C) and very high radiation exposure (> 150 dpa) is scarce. Experimental findings indicate a saturation of DBTT shifts as a function of dose, which could allow for long lifetime cladding operation. However, a strong increase in DBTT shift with decreasing irradiation temperature could compromise operation at low service temperatures.

Development of a deep understanding of the physics involved in the radiation damage mechanisms, together with multiscale computer simulation models of irradiation embrittlement will provide the basis to derive trendlines and quantitative engineering predictions.

List of Figures

Fig. 17: DBTT shift as a function of irradiation temperature for HT9 steel machined from the ACO_3 fuel duct irradiated to a dose of ~ 20.5 – 23.3 dpa in FFTF fast reactor [42].

Fig. 18: Comparison of DBTT shifts data [42].

Fig. 19: Comparison of USE data [42].

Fig. 20: Matrix of experimental data available on HT-9 DBTT shifts. Red lines indicate doses larger than 110 dpa and irradiation temperatures below 200^{o}C.

List of Tables

1. Introduction

Among the degradation mechanisms induced in steels by fast neutron irradiation, embrittlement is a major concern [3]. In particular, ferritic/martensitic (F/M) steels such as HT-9, are susceptible to brittle failure at low service temperatures. A measure of the steel brittleness is given by the ductile-to-brittle transition temperature (DBTT) shift and the change in the upper-shelf energy as a function of neutron exposure and irradiation temperature. The upper shelf energy (USE) is taken to be an indicator of the ductile fracture toughness. To determine DBTT, impact tests are performed on Charpy-V notch (CVN) specimens heated at different test temperatures in both the unirradiated and irradiated condition [4]. In the experiment, the amount of energy absorbed by the steel during fracture is determined. The Charpy impact energy-temperature curve is used to determine DBTT. Typically, the temperature at some arbitrary absorbed energy level is used as a measure of the transition temperature, e.g. 41 Joule (30 ft-lb) in a standard CVN test [5]. Irradiation embrittlement is usually characterized by the increase in DBTT, namely a shift in DBTT (ΔTT or ΔDBTT) and a decrase in USE. Exposure is typically measured in terms of fast fluence F(E > 1 MeV) or F(E > 0.1 MeV). Displacements per atom (dpa) is a better gauge of damaging-neutron exposure, because by definition it integrates the exposure over the entire neutron spectrum and gives a measure of the total energy deposited in the specimen during irradiation [6,7].

High-chromium F/M steels have been extensively investigated for applications in fast fission [2, 8, 9] and fusion reactor structures [10-12]. In the 1970s, 9-12%Cr steels were first considered for fast breeder fission reactors for fuel element cladding and core structural components. Stainless steels were commonly used at that time for in-core components. Radiation damage degraded the performance of these steels. In particular, neutron irradiation induced void swelling and creep, had a deleterious effect on dimensional stability, e.g. fuel subassembly bowing, dilatation, length increase, etc.

F/M steels offered a new avenue with specific advantages. F/M steels showed good properties of high swelling resistance to high dose in the temperature range 400-625^{o}C [13] and high creep strength to 550 – 600^{o}C [3], which made them attractive for use in the high temperature, high radiation regime of fast fission environments. High resistance to void formation (~1.02%) was observed in 12Cr-1MoVW steels during irradiations at 420^{o}C to doses up to 200 dpa [14-16]. Sandvik HT-9 steel (also known as 12Cr-1MoVW, DIN X20CrMoVW12 1) developed in Sweden was retained as candidate steel in the US fast reactor program. HT-9 was successfully used for driver subassembly structural components, fuel-pin cladding and wrappers/ducts in the Fast Flux Test Facility (FFTF) sodium-cooled fast breeder reactor. Alloy composition limits for HT-9 class of steels (Grade UNS Designation S42100) is given in ASTM A771 standard specification for Seamless austenitic and martensitic stainless steel tubing for liquid metal-cooled reactor core components, see Annex.

In the 1980s, experimental data for HT-9 steel was gathered from evaluations performed for fusion programs. Sandvik HT-9 was the first F/M steel

considered in the US Fusion Materials Program [12]. Fast reactor irradiations showed that swelling was not expected to limit the fusion first wall (FW) lifetime of 150-200 dpa, with the caveat that experiments in fast fission reactors could not account for the higher Helium and Hydrogen production rates present in FW and blanket structures.

At present, HT-9 has been retained for possible use in the Gen4 Module, a Gen4energy next generation fast reactor design (www.gen4energy.com). Gen4 Module is a small, modular nuclear reactor, formerly known as Hyperion Power Module (HPM) [17,18]. HPM is a uranium nitride fueled, lead-bismuth cooled nuclear reactor which has been designed to provide 25 Mw(e) for a 10-year lifetime without refueling. Fuel pellets are contained in HT-9 cladding tubes exposed to LBE core coolant temperatures ~ 500°C.

Radiation tolerance is a major factor in the selection of F/M steels as candidate cladding and structural materials in advanced fast fission and fusion reactors designs. As mentioned above, a most detrimental effect of neutron bombardment is radiation hardening and embrittlement manifested in a degradation of both DBTT and USE. To help in the prediction of irradiation effects on F/M impact properties, experimental data has been gathered in the past decades in several databases [5,19,20]. A good example of the difficulties involved in characterizing embrittlement behavior is summarized in Fig 1 where the importance of alloy composition and neutron spectrum effects is underlined [5].

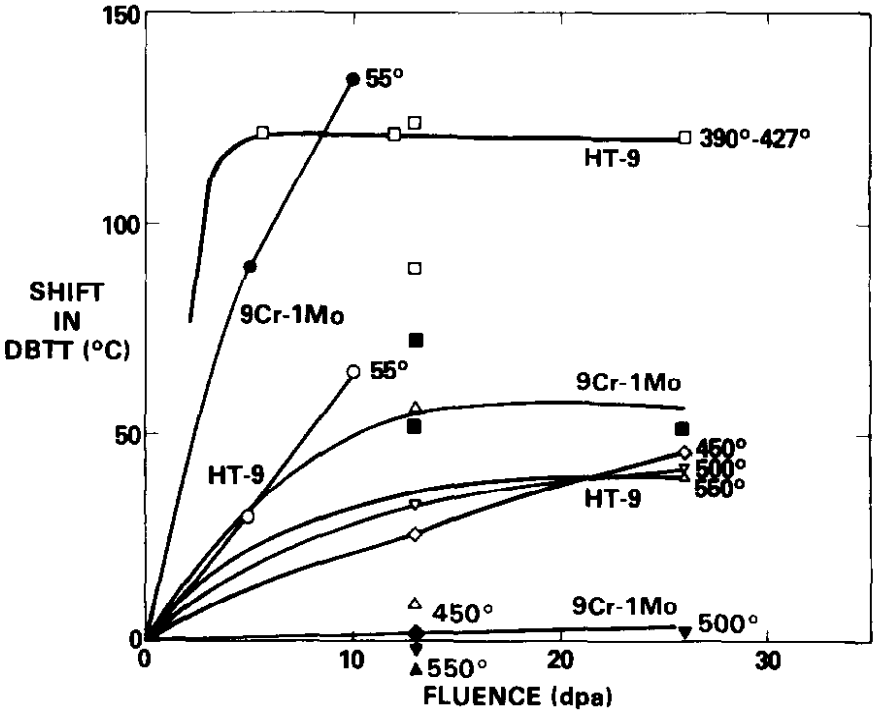

Fig. 1: DBTT shift in HT-9 as a function of fluence and temperature. HT-9 and 9Cr-1Mo steel irradiation response is compared [5].

In the figure, impact properties degradation is given as a function of neutron dose and temperature in two candidate F/M steels: HT-9 (Fe-12Cr-1Mo-0.2C- 0.5Ni-

0.5Mn-0.5W-0.2V) and Modified 9Cr-1Mo (Fe-9Cr-1Mo-0.1C-0.3V-0.15Nb). High irradiation temperatures in the range of 450°C – 550°C induce small shifts in both steels. HT-9 steel irradiated up to 26 dpa at 390-427°C shows large DBTT shifts (~ 140°C) that saturate at relatively low doses (~ 5 dpa). A concurrent reduction in USE of over 50% is observed [21]. At lower irradiation temperatures (55°C), tests performed on HT-9 steel in a different neutron spectrum show that saturation has not occurred after 10 dpa.

A significant difference in 9Cr-1Mo steel impact behavior is observed at low temperatures. At 55°C, the shift in 9Cr-1Mo is twice as large as that of HT-9, i.e. ~ 130°C at 10 dpa for 9Cr-1Mo (solid circles) as compared to 70°C for HT-9 (open circles). The authors point out that explanations for the observed behavior are not straightforward.

Clearly, extrapolations of impact properties to larger neutron dose or different temperature ranges outside the experimental database are not trivial, emphasizing the importance of understanding the physics behind the radiation damage mechanisms to help develop predictive trendlines. Future advanced reactor designs will make use of the collected database to infer mechanical properties for candidate steels with established operating windows. The big challenge is to predict materials irradiation response beyond these limits.

In an attempt to contribute to this end, we describe in the following section, selected irradiation embrittlement data found in the literature for HT-9 steel. The study reveals particular gaps in the empirical knowledge available. This report shows that for very low irradiation temperatures (< 200°C) and very high radiation exposure (> 150 dpa) data is scarce. Experimental findings indicate a saturation of DBTT shifts as a function of dose, which could allow for long lifetime cladding operation. However, a strong increase in DBTT shift with decreasing irradiation temperature could compromise operation at low service temperatures.

2. Embrittlement in HT-9 Steels

High fluence, high temperature data for HT-9 steel was gathered in the AD-2 EBR-II irradiation campaign that started August 1980 and ended April 1983. The chemical composition of the HT-9 heats used in the fabrications of specimens for the AD-2 experimental campaign is given in Table 1, taken from Puigh et al. [22].

Table 1: HT-9 chemical composition for heats 91353 and 91354 participating in AD-2 experiments in EBR-II [22].

ELEMENT	HT-9 (91353) Vendor[1]	HT-9 (91353) Overcheck[2]	HT-9 (91354) Vendor[1]	HT-9 (91354) Overcheck[2]
C	0.21	0.23	0.21	0.20
Mn	0.50	0.39	0.40	0.39
P	0.007		0.008	
S	0.003		0.003	
Si	0.22	0.21	0.21	0.14
Ni	0.58	0.46	0.58	3.49
Cr	11.80	12.34	12.11	12.39
Mo	1.02	0.99	1.03	0.99
V	0.32	0.45	0.33	0.45
Nb				
Ti	0.003		0.002	
Co			0.01	
Cu	0.04	0.07	0.00	0.07
Al	0.028		0.034	
B	<0.0010		0.0007	
As	<0.01		<0.005	
Sn				
Zr				
N	0.006		0.004	
O				
Pb				
Sb				
Ta	<0.01		<0.01	
W	0.50		0.53	
Fe	BAL.	BAL.	BAL.	BAL.

All numbers are weight percents.

[1]Carpenter Technology Certificate of Composition, dated July 22, 1975.

[2]Koon-Hall Test Report, dated August 21, 1979.

The purpose of the AD-2 experiment in EBR-II was to provide baseline mechanical property data for HT-9 steel evaluated for potential use in first walls and blanket of fusion reactors and for duct applications in liquid metal fast breeder reactors.

Experimental campaign, test matrix and irradiation conditions are described in [22-24]. In 1987, Hu et al. reported the analysis of AD-2 experimental findings on embrittlement response of HT-9 irradiated to high neutron dose [21]. Charpy tests were performed on V-notch precracked specimens (5 x 5 x 23.6 mm with a 0.76 mm deep notch). These specimens were obtained from HT-9 steel fabricated as follows:

1) HT-9 base metal from heat 91354 in a mill annealed condition (TT series). The bar stock was hot worked after soaking at 1149°C for a minimum of 1 h, slow cooled by allowed to transform to martensite, then tempered at 750°C for 1 h and air cooled (AC).
2) HT-9 base metal from heat 91354 (KT series), with a heat treatment of 1038 °C/10 min/AC + 760°C/30 min/AC

All specimens were fabricated from the same heat (91354) but received different heat treatment, with KT series having an annealing treatment at lower temperature (1038°C compared to 1149°C) for a shorter time (10 min compared to 1 h). Tempering was similar for both series (760°C for 30 min compared to 750°C for 1h).

Specimens of the TT series were fabricated from bar stock in the C-R orientation while specimens of the KT series were fabricated from plate stock with the crack plane oriented in the T-L direction. Specimens from the TT series were irradiated to ~ 26 dpa (6 x 10^{22} n/cm^2) and specimens from the KT series were irradiated to ~ 13 dpa (3 x 10^{22} n/cm^2). Irradiation temperatures were in the range of 390 to 550°C.

Shifts in DBTT were measured with respect to the non-irradiated condition (labeled “control” in Fig. 2) with DBTT defined as the inflexion point on the curve. Fig. 1 shows that lower irradiation temperatures induce larger shifts in DBTT in HT-9 (TT series) specimens.

Also, a net upper shelf energy (USE) reduction is observed, with the reduction being the same (53%) for all irradiation temperatures. After an irradiation to 26 dpa at a temperature of 390°C, the measured DBTT is 149°C (open circles) leading to a DBTT shift equal to 144°C. The DBTT shift for an irradiation at 550°C is only 41°C.

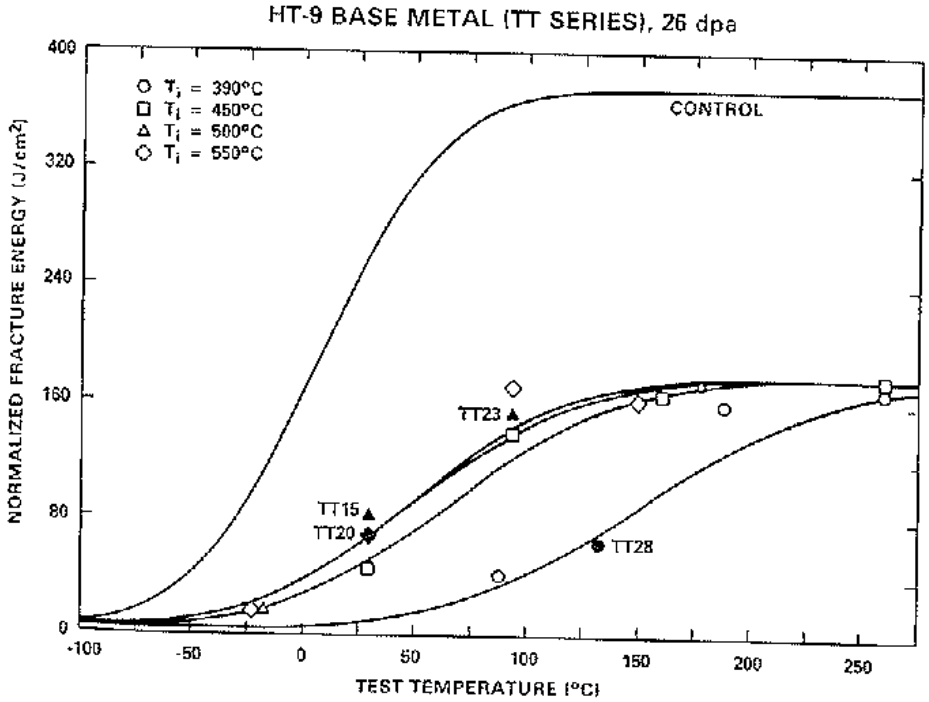

Fig. 2: Charpy impact test results on HT-9 base metal irradiated to 26 dpa [21].

Fig. 3 shows Charpy test results for HT-9 specimens (KT series) irradiated to lower fluence (13 dpa). A similar trend of larger DBTT shifts at lower irradiation temperatures and net decrease in USE is observed.

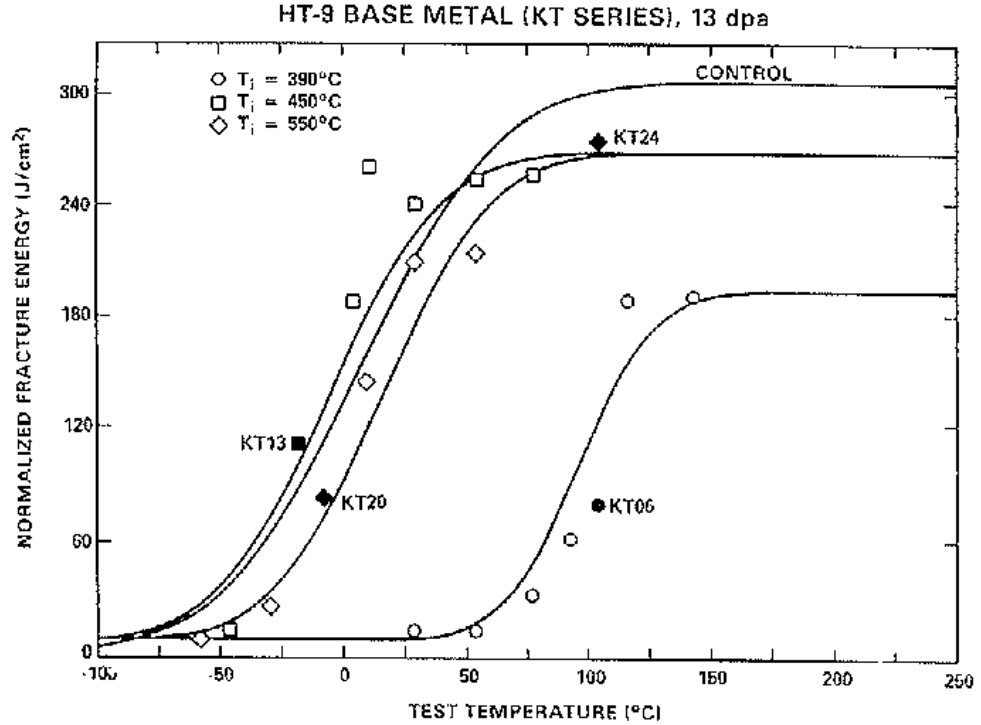

Fig. 3: Charpy impact test results on HT-9 base metal irradiated to 13 dpa [21].

As expected, the reduction of USE at 13 dpa is smaller reaching only 36% for the irradiation at the lowest irradiation temperature (390°C) or 12% for the irradiations at 450°C and 550°C. Lower neutron fluence translates into smaller DBTT shifts for a given irradiation temperature, e.g. at a temperature of 390°C the measured DBTT shift is only 89°C after exposure to 13 dpa (open circles in Fig. 3) while it is 144°C after exposure to 26 dpa (open circles in Fig. 2). Table 2 gives HT-9 DBTT and shift in DBTT as well as USE reduction for each irradiation condition shown in Figs. 2 and 3.

Table 2: Impact tests performed on HT-9 base metal after irradiation in EBR-II (AD-2 irradiation campaign) [21].

Dose (dpa)	Irradiation Temperature (°C)	DBTT (°C)	Shift in DBTT (°C)	USE reduction (%)
13	390	94	89	36
13	450	-8	-13	12
13	550	14	9	12
26	390	149	144	53
26	450	63	59	53
26	500	48	43	53
26	550	46	41	53

Note: DBTT is defined as the inflection point in the curves displayed in Figs. 2 and 3.

Effects of irradiation temperature and fluence on HT-9 DBTT shift are compared to those obtained for 9Cr-1Mo steel in Fig. 4.

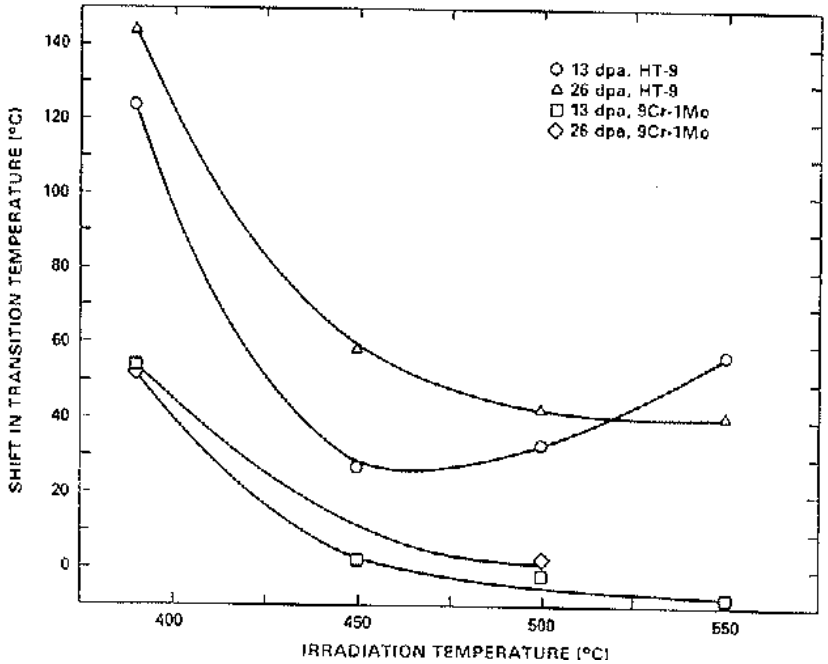

Fig. 4: Irradiation temperature and dose effects on DBTT shifts in HT-9 and 9Cr-1Mo [21].

Note that the shift in DBBT does not go to zero at 450, 500 and 550°C for HT9. This effect is attributed to precipitate coarsening during irradiation at high temperatures. The difference in behavior is attributed to different precipitate structure in HT-9 and 9Cr-1Mo.

The data reported in [21] suggest that 9Cr-1Mo steels show enhanced resistance to irradiation embrittlement. Lower DBTT shift at lower irradiation temperatures and lower DBTT shifts as a function of neutron dose is observed for 9Cr-1Mo as compared to HT-9 steels, as shown in Fig. 5. The figure indicates a possible saturation as a function of dose. A similar behavior has been observed in reactor pressure vessel (RPV) steels [25]. DBTT shift data obtained for RPV steels suggests that materials brittleness saturates at large fluence, DBTT shift has been found to follow a power law $\Delta TT \sim F(E > 1\ MeV)^n$; typically $n \sim 0.5$. Also, Charpy data obtained for RPV steels at very low dose suggest that as irradiation temperature decreases the shift in DBTT increases but saturates at maximum value of ~ 150°C [26].

Saturation of DBTT shift as irradiation temperature decreases has not been fully established in HT-9 steel. As shown in Fig. 5, irradiation experiments to larger fluence/dpa values are needed to establish a trend for HT-9.

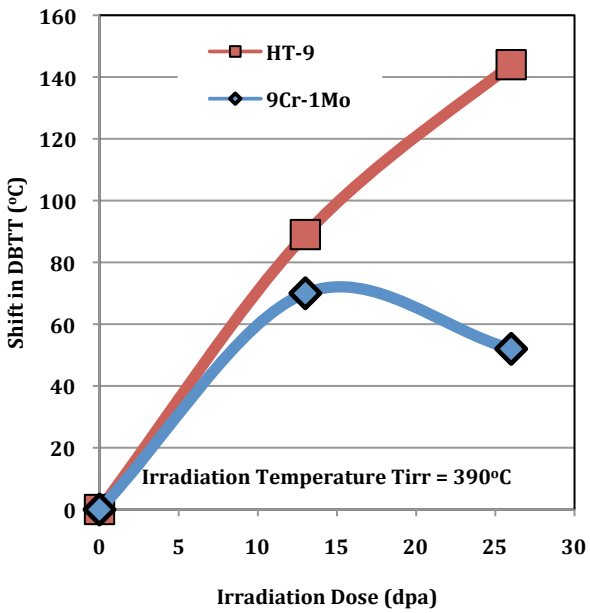

Fig. 5: Neutron exposure effects on DBTT shifts are larger in HT-9 than 9Cr-1Mo irradiated at the same low irradiation temperature (390°C).

Experimental data reported in Fig. 4 show that the maximum DBTT shift observed in HT-9 specimens is 144°C for the worst-case scenario, i.e. at the lowest irradiation temperature (390°C) and the highest exposure (26 dpa). Fig. 4 emphasizes the relevance of experimental data obtained at lower irradiation temperatures (T_{irr} < 390°C) and higher fluence values (> 26 dpa).

Results reported in Figs. 2-4, confirmed previous investigations performed by Hu in 1981. As shown in Fig. 6, similar low temperature embrittlement irradiation response was obtained in previous Charpy tests performed on HT-9 base metal irradiated in EBR-II at temperatures in the range 390°C and 550°C and 13 dpa [27]. Specimens irradiated at 390, 450, 500 and 550°C have a shift in DBTT of 124, 27, 33 and 57°C, respectively and ~ 40% average reduction in USE.

Table 3: Impact tests performed on HT-9 base metal after irradiation in EBR-II [27].

Dose (dpa)	Irradiation Temperature (°C)	DBTT (°C)	Shift in DBTT (°C)	USE reduction (%)
13	390	129	124	49
13	450	31	27	35
13	500	37	33	36
13	550	61	57	43

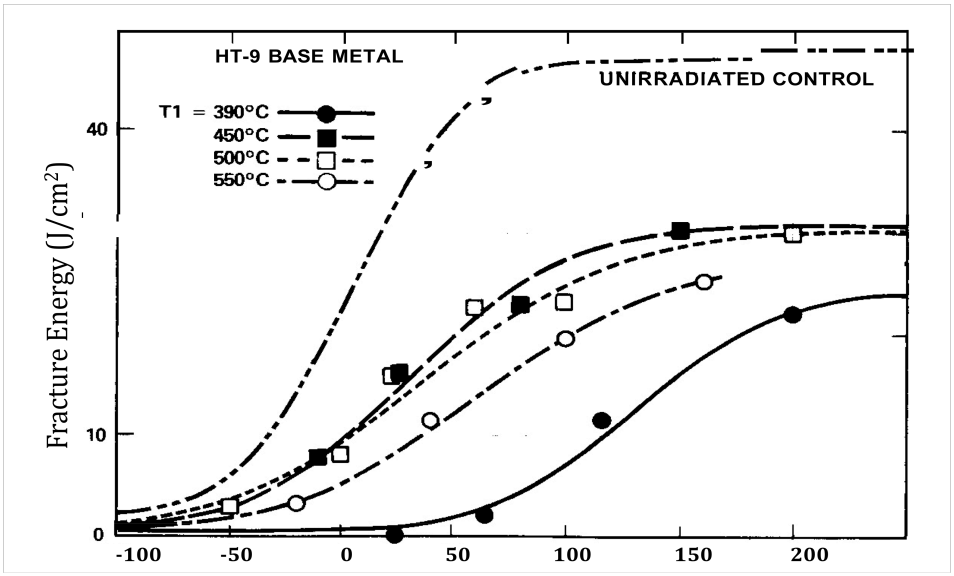

Fig. 6: DBTT measurements as a function of test temperature in HT-9 base metal irradiated in EBR-II to 13 dpa [27]

Fig. 7 gives a summary of the effects of irradiation temperature on HT-9 DBTT shift after irradiation to 13 dpa obtained by Hu et al. [21, 27]. The embrittlement behavior is similar with lower irradiation temperatures inducing larger shifts in DBTT. The differences that appear could be linked to HT-9 fabrication/processing; according to the authors these might have played a role in the embrittlement response of HT-9 steel.

.

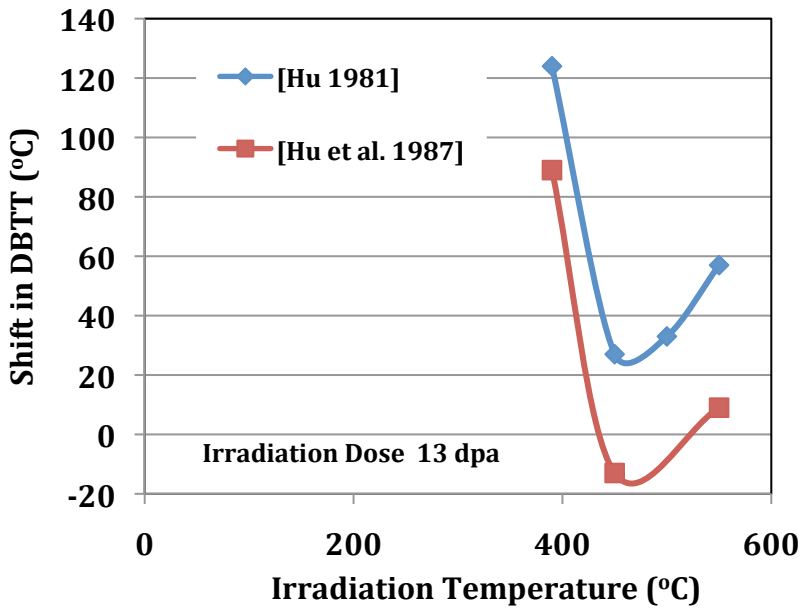

Fig. 7: Shifts in DBTT in HT-9 steel irradiated at 13 dpa. The difference in HT-9 steel response could be ascribed to different thermal treatment with a possible effect of the rolling direction [21,27].

In 1981, Hu also obtained Charpy data for welds [27]. Properties of welds under irradiation were shown not to change significantly. Welds and heat affected zone (HAZ) DBTT response under irradiation was investigated at temperatures of 390, 450, 500, and 550°C to a dose of 13 dpa. It was observed that DBTT of welds and HAZ where the same or slightly lower than that of the base metal [27]. This result indicated that HT-9 steel could be used in fusion first wall applications without suffering a major degradation in performance due to the presence of welds.

In 1987, Corwin et al. [28] reported impact test results of 12Cr-1MoVW steel irradiated in the fast spectrum EBR-II reactor to comparable dose (~ 12 dpa) with Helium levels < 1 ppm obtaining results similar to those reported by [21]. The chemical composition of 12Cr-1MoVW (heat XAA-3587 containing 0.43% Ni) used in these experiment is given in Table 4. Note that heat XAA-3587 conforms to ASTM 771 standard, which specifies Ni 0.30-0.80wt% for this class of steels (S42100). Heat XA-3587 was prepared by Combustion Engineering, Inc. Chattanooga, Tennessee. Other heats with 1% and 2%Ni content also participated in the experiment.

Nominal heat treatment of normalizing and tempering conditions were selected, i.e. 30 min at 1050°C/air cooled (AC) followed by 2.5h at 780°C/AC. Half-size specimens were used in the experiment. DBTT was determined based on the 5.5-J index, which corresponds after volumetric scaling to the indexing values of 41 J [29].

Table 4: Composition of 12Cr-1MoVW heats of steel used in impact tests performed after irradiation in EBR-II to 12 dpa [28].

Element	Concentration (wt%) [a]				
C	0.21	Mo	0.93	B	< 0.001
Mn	0.50	V	0.27	W	0.54
P	0.011	Nb	0.018	As	< 0.001
S	0.004	Ti	0.003	Sn	0.002
Si	0.18	Co	0.017	Zr	< 0.001
Ni	0.43	Cu	0.05	N	0.020
Cr	11.99	Al	0.030	O	0.005

[a] Balance iron.

Fig. 8 and Table 5 show that irradiation at 390°C to a fluence F(E > 0.1 MeV) ~ 2.5 x 10^{26} n/m^2 which corresponds to a displacement damage of ~12 dpa produced a shift in DBTT of 127°C in 12Cr-1MoVW. Also, a decrease in USE from 26 J to 13 J is observed.

Two groups of specimens were prepared to separately study thermal aging and irradiation effects. A group of specimens was aged at temperatures similar to the irradiation temperature for aging times similar to the irradiation time.

As shown in Fig. 8, only minor aging effects are found. After aging 12Cr-1MoVW steel at 400°C for 5000 h impact tests results indicate a shift in DBTT of only 14°C. The authors report that addition of Ni was found not to significantly influence radiation induced changes.

Table 5: Impact tests performed on 12Cr-1MoVW steel before and after irradiation in EBR-II to 12 dpa at 390°C [28].

Dose (dpa)	Irradiation Temperature (°C)	DBTT (°C)	Shift in DBTT (°C)	Indexed at	USE
0		-58			26
12	390	92	127	5.5 J	13

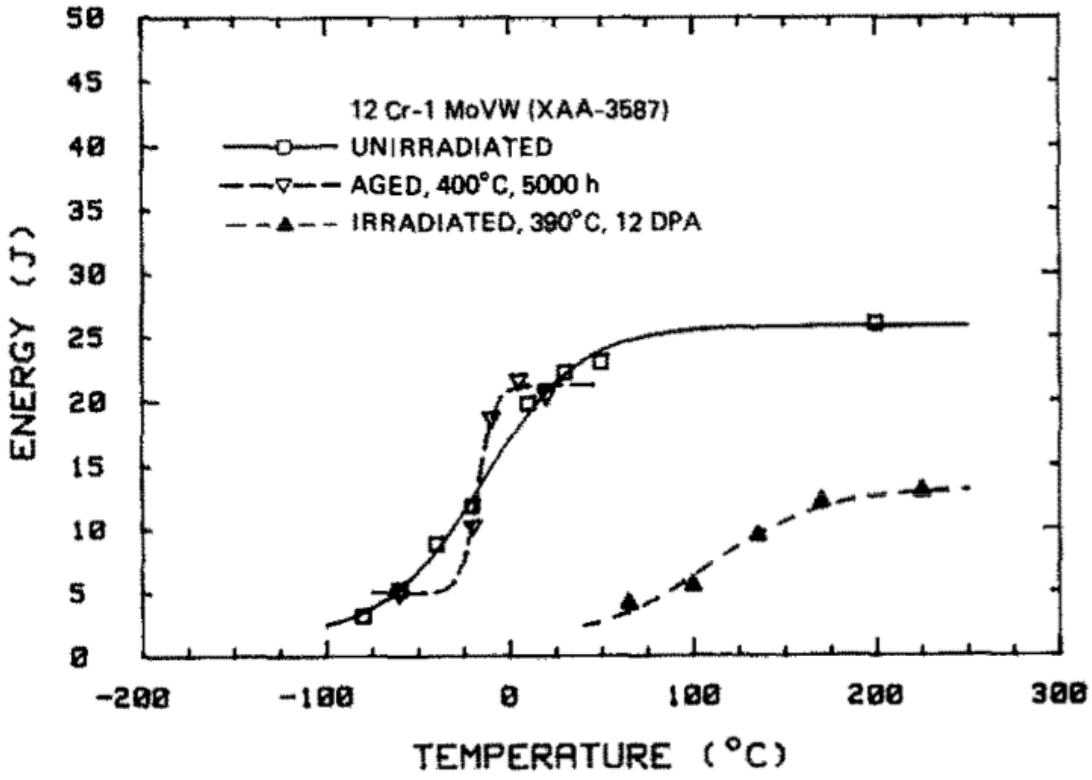

Fig. 8: Impact tests in 12Cr-1MoVW (XAA-3587) steel in the unirradiated and annealed conditions and irradiated at 390°C to 12 dpa in EBR-II [28].

HT-9 base metal DBTT response for larger dose values was reported in 1994 [30]. Chemical composition of HT-9 steel used in this investigation is reported in Table 6 [31].

Table 6: Chemical composition of HT-9 steel irradiated in Phenix to 110 dpa and temperatures in the range of 400-520°C [31].

	C	Cr	Mo	Mn	Si	Ni	V	Nb	W
HT 9	0.19	12.0	0.96	0.6	0.42	0.56	0.3	–	0.54

According to the authors, HT-9 normalization at 1050°C/30 min followed by tempering at 780°C/2.5h lead to a fine lath martensitic structure. HT-9 Charpy specimens (length 55 mm, width 10 mm, thickness 3.5 mm) were machined in the longitudinal (L) and transversal (T) direction of cold rolling. Fig. 9 illustrates the irradiation temperature dependence of DBTT measured in HT-9 steel exposed to a dose of 110 dpa in Phenix reactor. Values given in Table 7 are taken from Fig. 9. These results agree with previous observations, i.e. lower irradiation temperatures lead to larger shifts in DBTT.

Table 7: Results of impact tests performed on HT-9 steel irradiated in Phenix to 110 dpa and temperatures in the range of 400-520°C [31].

Dose (dpa)	Irradiation Temperature (°C)	$DBTT_0$ (°C)	DBTT (°C)	Shift in DBTT (°C)	Orientation
110	400	-42	115	157	T
110	520	-42	43	85	T
110	420	-40	57	97	L
110	470	-40	22	62	L

In Fig. 9, HT-9 response can be compared to that of different F/M steels (HT-9, T91, EM10, EM12, F17, and 1.4914) also irradiated in Phenix to different doses. HT-9 steel in the L-orientation (open squares) shows the highest DBTT value of ~ 115°C, corresponding to the highest shift in DBTT; i.e. ~157°C after exposure to 110 dpa at an irradiation temperature of 400°C. Note the poor embrittlement response of the fully ferritic unstabilized F17 (17Cr, 0.06C) irradiated to 91 dpa with the largest DBTT values (dashed line). The authors underline the particularly good behavior of fully martensitic EM10 steel (8.8 wt% Cr), which shows DBTT values that are always below room temperature (bottom dotted line).

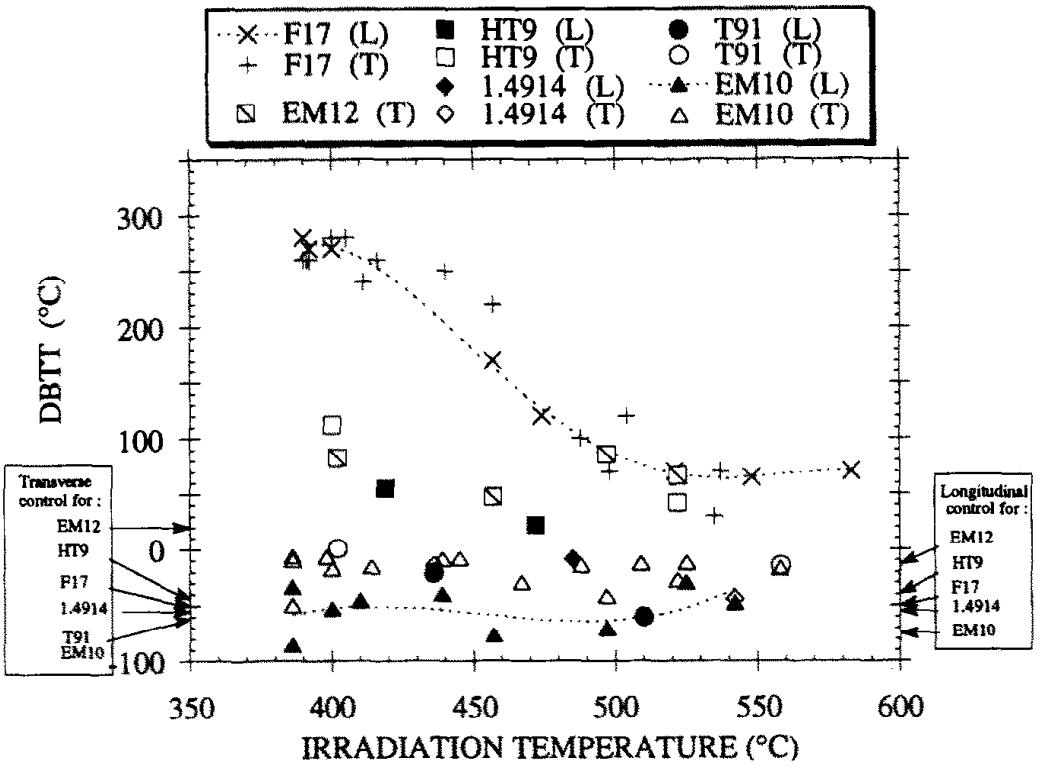

Fig. 9: DBTT as a function of irradiation temperature for HT-9 steel irradiated to a dose of 110 dpa in Phenix fast breeder reactor [30]. Doses for other steels are 91 dpa for F17, 33 dpa for EM12, 109 dpa for 1.4914, 68 dpa for T91 and 97 dpa for EM10.

Embrittlement effects, measured in terms of DBTT shift, tend to vanish as irradiation temperature increases, e.g. Fig. 10 shows that after irradiation to 110 dpa in Phenix reactor, DBTT shift for HT-9 in the L-orientation is only ~43°C when irradiated at 520°C and increases to ~157°C when irradiated at 400°C.

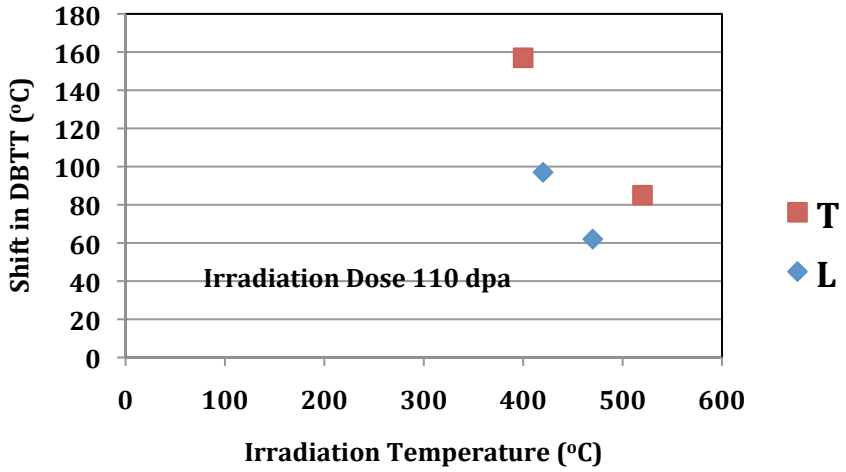

Fig. 10: Effect of irradiation temperature on DBTT shift in HT-9 specimens in T and L orientation irradiated in Phenix reactor to 110 dpa.

12Cr-1MoVW steel specimens were also irradiated in materials testing reactors (MTS) such as the High Flux Isotope Reactor (HFIR) [32,33]. Irradiations at 400°C to a dose of ~ 40 dpa produced shifts in DBTT of 242°C. The very large shift obtained is attributed to the high helium concentration generated during the irradiation under HFIR mixed-spectrum.

A fast reactor has a "harder" neutron spectrum, i.e. only small amounts of helium (< 1 appm) will form in 12Cr-1MoVW steels in a fast reactor. The question could be raised on how representative irradiations in MTS reactors are to evaluate steel embrittlement in fast reactors. Note that ASTM guidelines for RPV's embrittlement determination recommend the use of DBTT shifts obtained from surveillance specimen Charpy V-notch tests.

As mentioned above, experiments at low irradiation temperatures are of crucial importance to determine safe operation at low service temperatures. Experiments at 365°C were performed in the Fast Flux Test Facility FFTF [34]. Specimens were irradiated in the materials open test assembly (MOTA). Charpy tests were performed on half-size specimens of normalized and tempered HT-9 steel (heat 9607-R2) with chemical composition given in Table 8.

Table 8: Chemical composition of HT-9 steel irradiated in FFTF to 10 and 17 dpa at an irradiation temperature T = 365°C [34].

12Cr-1MoVW (Heat 9607-R2)			
C	0.20	Ni	0.51
Si	0.17	V	0.28
Mn	0.57	W	0.45
P	0.016	N	0.027
S	0.003	Al	0.006
Cr	12.1	Ti	0.001
Mo	1.04	Cu	...

Fig. 11 and Table 9 show the results obtained after exposure to 10 and 17 dpa. A shift in DBTT of 161°C is obtained for both fluence values indicating saturation in the shift with increasing fluence.

Table 9: Results of impact tests performed on half size specimens of HT-9 steel irradiated in FFTF to 10 and 17 dpa and 365°C [34].

Dose (dpa)	Irradiation Temperature (°C)	$DBTT_0$ (°C)	DBTT (°C)	Shift in DBTT (°C)	USE (J)
0		**-19**			**20.8**
10	365		142	161	11.4
17	365		142	161	10.0

In general, impact values of DBTT obtained with half-size specimens are not always directly comparable to those from standard-sized specimens (length 10 mm, width 10 mm, thickness 50 mm). Note that in the case of 12Cr-1MoVW steels [5, 28, 34] and in RPV steels [35] the shift in DBTT has been found not to be sensitive to specimen size and geometry. Therefore, the impact energy data depicted in Fig. 11 is valuable for trendline assessments.

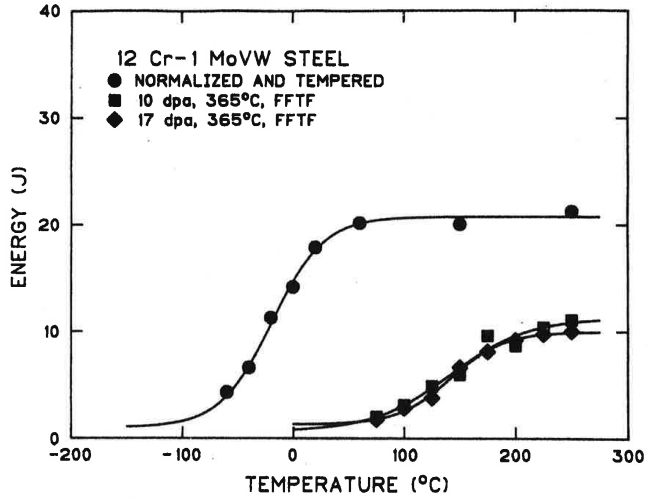

Fig. 11: Charpy curves for half-size specimens of 12Cr-1MoVW steel before and after irradiation to 10 and 17 dpa at 365°C in FFTF [34].

Similar DBTT shifts were obtained for HT-9 specimens irradiated in EBR-II to ~ 6 dpa at an irradiation temperature of 427°C [36]. Specimens were fabricated from 3.3 cm diameter HT-9 rod stock from Carpenter Technology. The HT-9 (melt 91354) chemical composition is given in Table 10. Heat treatment consisted of solution anneal at 1050°C for 30 min/AC and tempering at 780°C for 2.5 h/AC. The authors mention that this heat treatment is considered representative of commercial practice for HT-9 for high temperature service.

Table 10: Chemical composition of HT-9 (91354) steel irradiated in EBR-II to ~ 6 dpa at an irradiation temperature T = 427°C [36].

Element	HT-9 Rod (91354)
Cr	12.09
Mo	1.02
C	.21
Mn	.50
Si	.21
P	.008
S	.003
Ni	.58
V	.33
W	.54

During the experiment, samples were in direct contact with the EBR-II reactor coolant (flowing sodium). Impact test results for the irradiated and non-irradiated condition are shown in Fig. 12. Open circles correspond to the non-irradiated as-received condition. Open triangles correspond to impact tests of specimens irradiated in EBR-II after an exposure to F(E > 0.1 MeV) ~ 1 x 10^{22} n/m^2 (~ 6 dpa) at 427°C. A DBTT shift of 108°C is observed from Charpy impact energy-temperature curves indexed at 41 J absorbed energy. This shift is similar to previous findings. USE decrease is also observed.

Also, impact tests on specimens thermally aged for 5000 h are shown in Fig. 12 for two different aging temperatures 427°C (solid circles) and 538°C (solid squares). As indicated in Fig. 10, aging to 538°C for 5000 h induced a shift in DBTT of ~ 39°C. Extension to 11,000 h of aging time produced no further shift in the transition temperature.

Table 11: Results of impact tests performed on full size specimens of HT-9 (91354) steel irradiated in EBR-II to 6 dpa at 427°C [36].

Dose (dpa)	Irradiation Temperature (°C)	Shift in DBTT (°C)	Indexed at
6	427	108	41 J

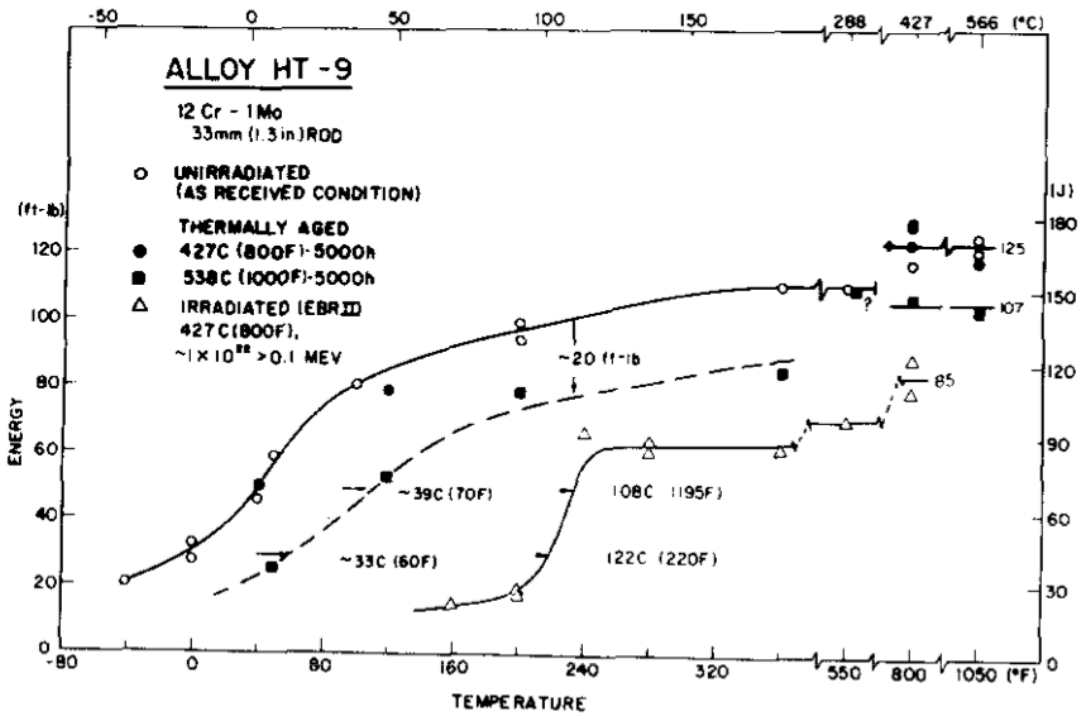

Fig. 12: Charpy curves of full size specimens of Alloy HT-9 Rod in as-heat treated, thermally aged and irradiated condition [36].

In general, experimental findings suggest that changes in DBTT for HT-9 begin to saturate at relatively low fluences [26]. Fig. 13 shows that at irradiation temperatures of 390°C (solid circles) after 15 dpa the slope of the curve begins to decrease as fluence increases and at 30 dpa there is only a slight positive slope indicating that saturation is occurring.

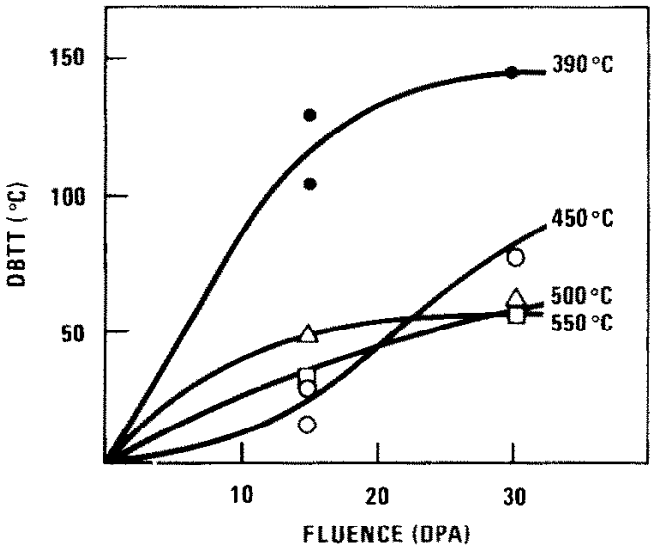

Fig. 13: Effect of irradiation temperature and fluence on DBTT of 12Cr-1MoWV. Lower temperatures of 390°C (solid circles) increase the DBTT more than temperatures above 500°C (open triangles and squares)[26].

In 1992, Klueh et al. [37] investigated the effect of different normalizing-and-temperature treatments on 12Cr-1MoVW impact properties. The 12Cr-1MoVW steel was taken from an AOD/ESR melt that was processed into hot-rolled plate (heat 9607-R2) with chemical composition given in Table 8. The steel plates (88.9 x 152 x 9.5 mm) followed four different heat treatments, i.e. normalization at 1040°C for 1 h/AC followed by tempering at 780°C for 1h/AC and 780°C for 2.5 h/AC, and normalization at 1110°C for 1 h/AC followed by tempering at 780°C for 1h/AC and 780°C for 2.5 h/AC.

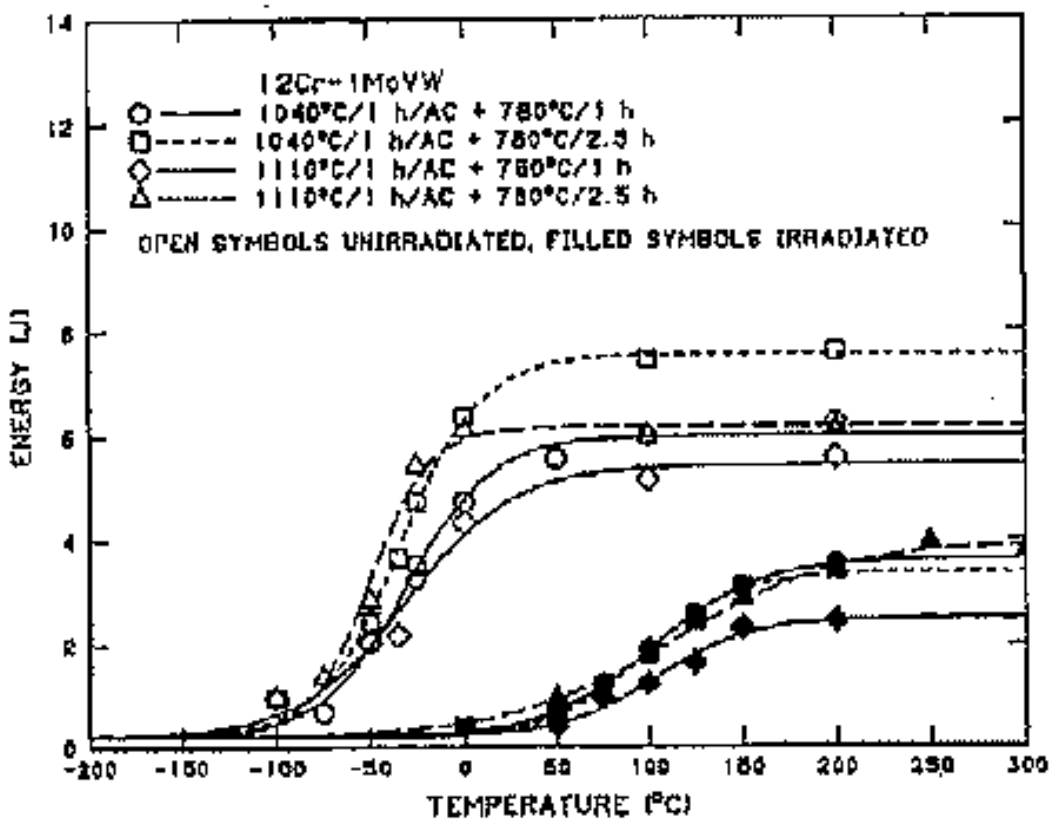

Fig. 14: Charpy curves for 12Cr-1MoVW steel (heat 9607-R2) in as-heat treated and after irradiation to 4 dpa at 365°C in FFTF reactor [37, 38].

Irradiations were performed in FFTF reactor (MOTA 1E experiment). 12Cr-1MoVW steel was irradiated to a fluence F(E > 0.1 MeV) 1.1 x 10^{26}n/m^2 (~ 4 dpa) at 365°C. Charpy tests performed on 12Cr-1MoVW steel (heat 9607-R2) with different heat treatments showed essentially no differences in DBTT shifts. Table 12 and Fig. 14 display impact tests results. The investigation shows that the shift in DBTT is relatively independent of heat treatment. The USE was essentially the same for all four heat treatment conditions after irradiation.

Table 12: Results of impact tests performed on 12Cr-1MoVW steel (heat 9607-R2) steel irradiated in FFTF reactor to 4 dpa at 365°C [37].

Dose (dpa)	Irradiation Temperature (°C)	$DBTT_0$ (°C)	DBTT (°C)	Shift in DBTT (°C)	USE_0 (J)	USE (J)	Delta USE J (%)	Heat Treatment
4	365	-32	97	129	6	3.6	-2.4 (40)	1040/1h/AC; 760/1h
4	365	-35	95	130	7.6	3.4	-4.2 (55)	1040/1h/AC; 780/2.5h
4	365	-34	100	134	5.4	2.5	-2.9 (54)	1100/1h/AC; 760/1h
4	365	-51	107	157	6.2	3.9	-2.3 (37)	1100/1h/AC; 780/2.5h

Similar conclusions were derived from 12Cr-1MoVW steels irradiated at 420°C in FFTF reactor (MOTA) [38]. One-third-size Charpy specimens (3.3 x 3.3 x 25.4 mm) in L-T orientation were fabricated from 12Cr-1MoVW steels (9607-R2) with two different heat treatments. Heat treatments consisted in normalization at 1040°C for 1h/AC followed by two different tempering, i.e. at 760 for 1h and 780°C for 2.5 h. Specimens tempered at 760 and 780°C were exposed to 7.4 and 7.8 10^{26} n/m^2 (34 and dpa), respectively. As shown in Fig. 15 and Table 13, results obtained show no significant effect of heat treatment on 12Cr-1MoVW DBTT shifts.

Table 13: Results of impact tests performed on 12Cr-1MoVW steel (9607-R2) steel irradiated in FFTF reactor to ~ 35 dpa at 420°C [38].

Dose (dpa)	Irradiation Temperature (°C)	$DBTT_0$ (°C)	DBTT (°C)	Shift in DBTT (°C)	USE_0 (J)	USE (J)	Delta USE J (%)	Heat Treatment
34	420	-32	55	87	6	4.1	-1.9 (32)	1040/1h/AC ; 760/1h
36	420	-35	72	107	7.6	4.1	-3.5 (46)	1040/1h/AC ; 780/2.5h

The investigation suggested that a tempering temperature lower than the 780°C could be beneficial in reducing the effect of irradiation on DBTT in 12Cr-1MoVW steel. Also, based on the studies of Little et al. [13] lower carbon content steel was found to induce a much finer precipitate distribution in a 12Cr-0.9Mo-0.3V-0.14 C steel with possible significant effects in DBTT.

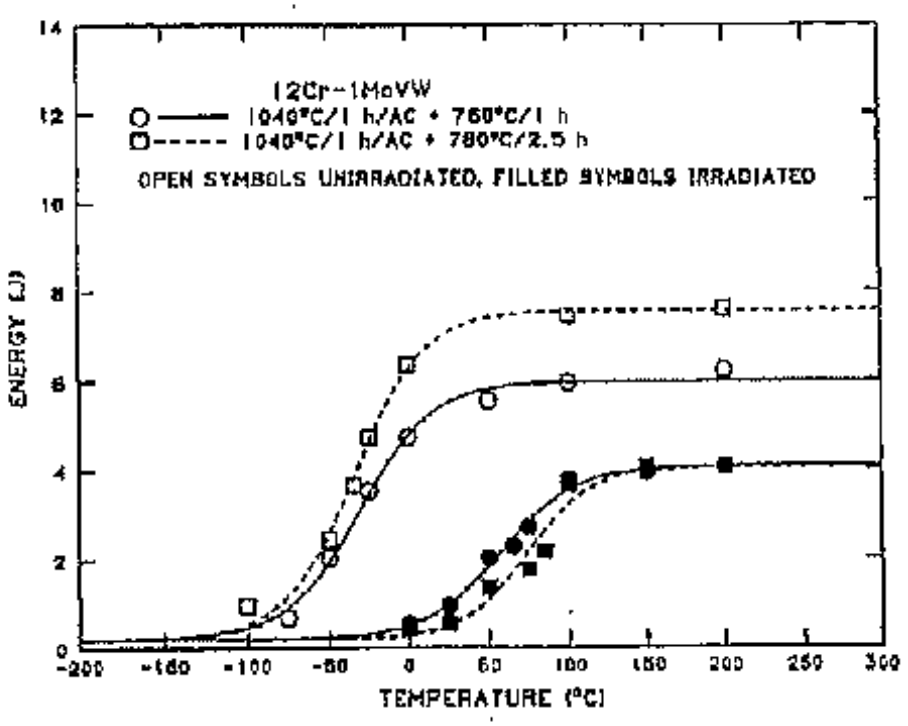

Fig. 15: Charpy curves for 12Cr-1MoVW steel (heat 9607-R2) in as-heat treated and after irradiation to ~35 dpa at 420°C in FFTF reactor [38].

Results of Charpy tests have been reported for HT-9 steel irradiated at 200°C in BR2 reactor in SCK.CEN, Belgium [39, 40]. Irradiations were performed within the framework of the Euratom FP-5 SPIRE project. HT-9 chemical composition is listed in Table 14. HT-9 material was provided by Aubert-Duval (orig. denomination: 56 B.I.).

The steel was normalized at 1050°C/30 min and tempered at 700°C/2h. Specimens were irradiated in the Multipurpose Irradiation System for Testing of Reactor Alloys (MISTRAL) rig with the purpose of studying irradiation effects on high chromium F/M steels for MYRRHA project; a lead-bismuth cooled experimental accelerator driven system (ADS) [41, http://myrrha.sckcen.be/].

Table 14: HT-9 steel chemical composition irradiated in BR2 reactor [39].

C	Ni	Cr	Mo	Si	S	V
0.204	0.66	11.68	1.06	0.45	<0.003	0.29
Ti	**N**	**P**	**Mn**	**B**	**W**	**Nb**
		0.020	0.63		0.47	0.03

As shown in Fig. 16 and Table 15, DBTT equals 169°C for the irradiation to a dose of ~ 3.7 dpa and 163°C for the irradiation at 2.47 dpa. The authors report a USE reduction of 41% for the largest dose of ~ 3.7 dpa and 37% for the irradiation

at 2.47 dpa. HT-9 DBTT shift is compared with the shifts obtained under similar conditions of dose (2.43-2.91 dpa) and same irradiation temperature (200°C) for EM10 and T91 steels and conclude that HT-9 shows the largest embrittlement, with DBTT shifts equal to 168°C, 109°C, and 84°C, for HT-9, T91 and EM10, respectively.

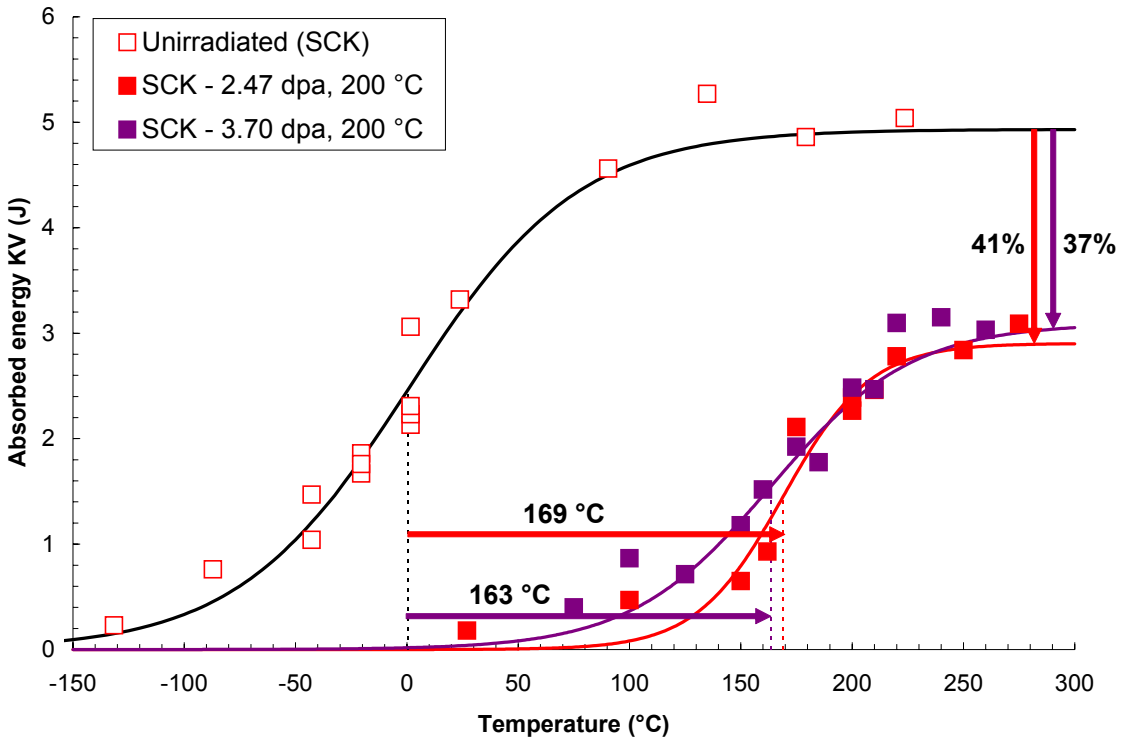

Fig. 16: Effect of irradiation temperature on DBTT shift in HT-9 specimens irradiated in BR2 reactor to 2.47 and 3.7 dpa at an irradiation temperature of 200°C [39].

Table 15: Results of impact tests performed on HT-9 steel steel irradiated in BR2 reactor to ~ 2.47 and 3.7 dpa at 200°C [39,40].

Dose (dpa)	Irradiation Temperature (°C)	DBTT (°C)	Shift in DBTT (°C)	USE J(%)
0	200	1		4.9
2.47	200	169	168	2.9 (41)
3.7	200	163	162	3.1 (37)

One of the last experiments run in FFTF (consisting of HT-9 clad oxide fuel and an HT-9 duct) was called the ACO-3 experiment [43]. ACO-3 duct was exposed to a wide range of irradiation doses 3-148 dpa and temperatures 378-504°C. ACO-3 duct (heat #84,4250) heat treatment consisted of normalizing at 1065°C 30min/AC followed by tempering at 760°C 1h/AC.

New data for HT-9 steel irradiation response has recently been reported in 2012 [42]. HT-9 subsize steel specimens were machined from the ACO-3 duct irradiated in FFTF reactor. Impact tests were also performed on archive material. The change in DBTT for ACO-3 duct HT-9 specimens in the L-T orientation is depicted in Fig. 17 (black diamonds) and Table 16. Archive material for T-L orientation was not available so only shifts in DBTT in L-T orientation were determined. A strong dependence on irradiation temperature is observed. In Fig. 17, DBTT shifts monitored from Charpy impact energy-temperature curves indexed at two other different absorbed energies are also reported, namely 1 J (red triangles), 2 J (blue circles). At the lowest irradiation temperature of 380 or 383 ^{o}C, DBTT shifts equal to 237, 258 and 218^{o}C are observed for a total dose of ~ 20.5 dpa or 23.3 dpa.

Table 16: DBTT shifts in HT-9 steel from ACO-3 duct irradiated in FFTF [42].

Dose (dpa)	Irradiation Temperature (°C)	Shift in DBTT (C)	Orientation	Indexed at
20.5/23.3	380/383	258	L-T	2 J
		237	L-T	1 J
		218	L-T	41 J

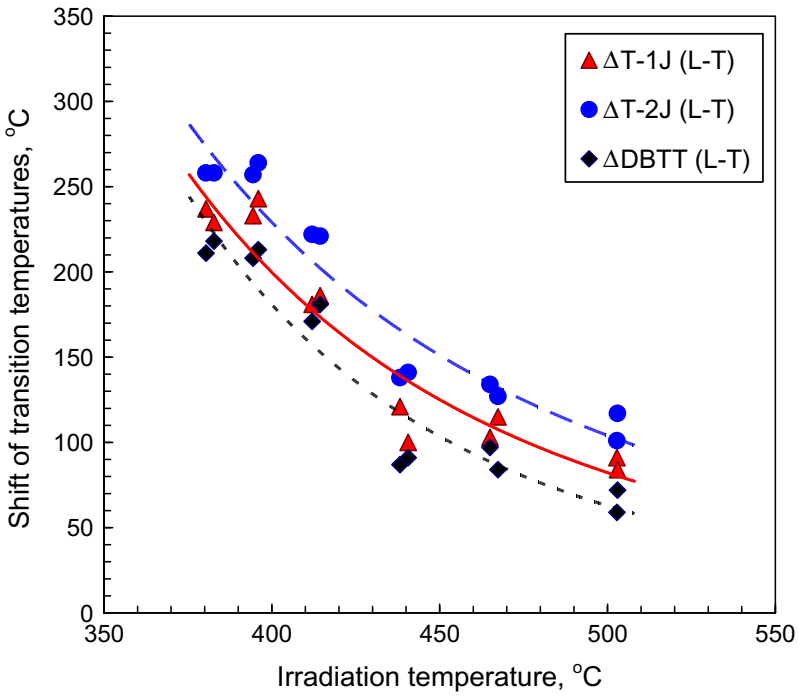

Fig. 17: DBTT shift as a function of irradiation temperature for HT9 steel machined from the ACO_3 fuel duct irradiated to a dose of ~ 20.5 – 23.3 dpa in FFTF fast reactor [42].

As shown in Fig. 18, DBTT shifts obtained from subsize ACO-3 duct specimens are consistent with data from earlier studies. The dotted line encloses the highest DBTT shifts. Except for the data mentioned in Fig. 16 obtained in SCK.CEN Belgium, very few data points exist below 300°C and extrapolation of DBTT shift values in the low temperature range becomes difficult. Note in particular, the solid blue circles, labeled as "This Study" that correspond to DBTT shifts as a function of irradiation temperature for HT9 steel machined from the ACO_3 fuel duct irradiated to a dose of ~ 3-148 dpa in FFTF fast reactor. These results suggest a drastic drop in DBTT shift at irradiation temperatures above 450°C.

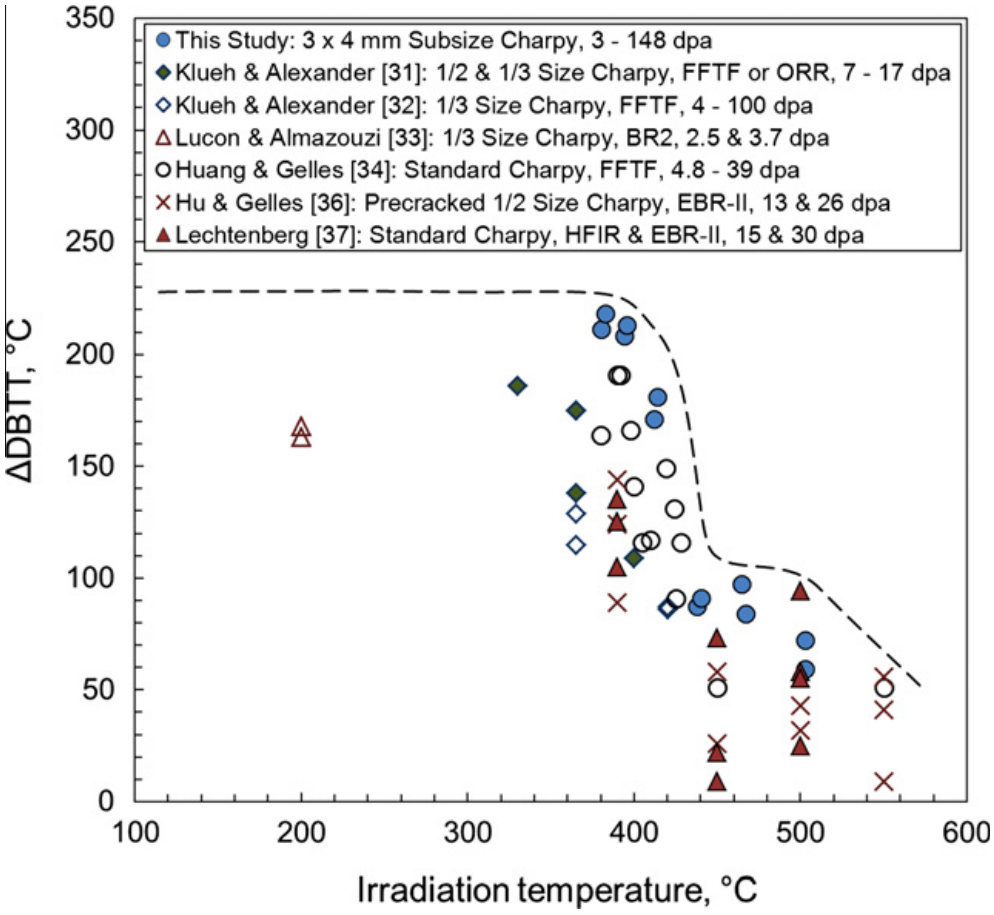

Fig. 18: Comparison of DBTT shifts data [42].

Irradiation temperature dependences of USE were found not to be significant, as shown in Fig. 19. Dotted lines enclose the maximum and minimum values, except for two data points corresponding to tests performed on pre-cracked Charpy specimens. The authors conclude that USE reduction was similar for all cases regardless of differences in materials and irradiation conditions.

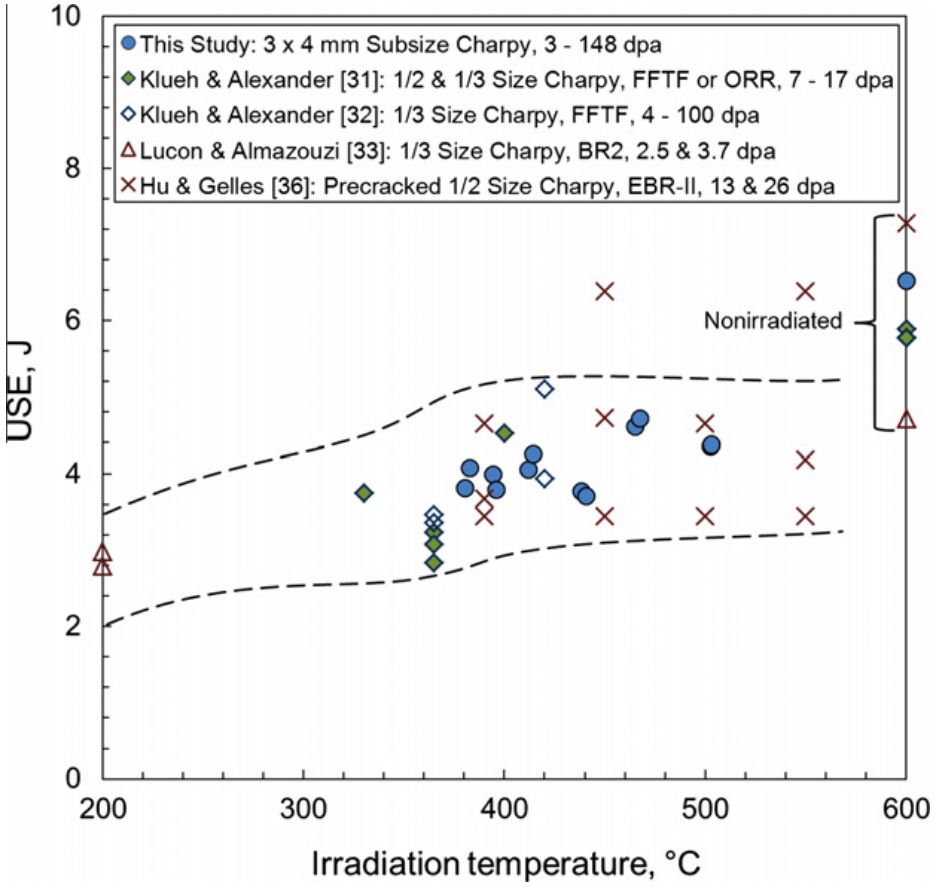

Fig. 19: Comparison of USE data [42].

HT-9 steels data gathered over the past decades complemented with recent experimental findings provide a significant starting point in the analysis of mechanical properties degradation under irradiation. In this report, we have considered only one aspect, i.e. HT-9 embrittlement because of its importance in defining the lower operating temperature limit in the next generation of fission nuclear reactor. Extensive data is also available in HT-9 materials properties database to describe the upper temperature limit given by irradiation and thermal creep and corrosion in liquid coolants. This effort contributes to the development of ASME codes for irradiated conditions.

Conclusions

Table 17 displays the DBTT shifts discussed in this report. The matrix shows that the trend observed by several authors is confirmed, i.e. the largest DBTT shift values are found at the lowest temperatures and DBTT shift values decrease as irradiation temperature increases.

Table 17: DBTT shifts reported in the literature described in this report.

T_{irr}(°C) Dpa	200	200	365	380	390	400	420	427	450	470	500	520	550
2.47	169												
3.7		163											
4			129										
4			130										
4			134										
4			157										
6								108					
10			160										
12					127								
13					124								
13					89								
13											33		
13													57
13													9
13									27				
17			160										
26					144								
26									59				
26											43		
26													41
34							87						
36							107						
110						157							
110							97						
110										62			
110												85	

As schematically depicted in Fig. 20, the experimental data on DBTT shifts described in this report is limited to irradiation temperatures above 200°C and dose values below 110 dpa. The data covers the region of fast reactor operating temperatures (350-550°C) for doses below 50 dpa.

Data at low irradiation temperatures and/or large irradiation dose are needed to define trendlines. Exceptional datapoints have been reported at 110 dpa, or at low irradiation temperatures ~ 200°C. Data at low irradiation temperatures is

of particular importance since low temperature embrittlement could result in steel failures during off normal events.

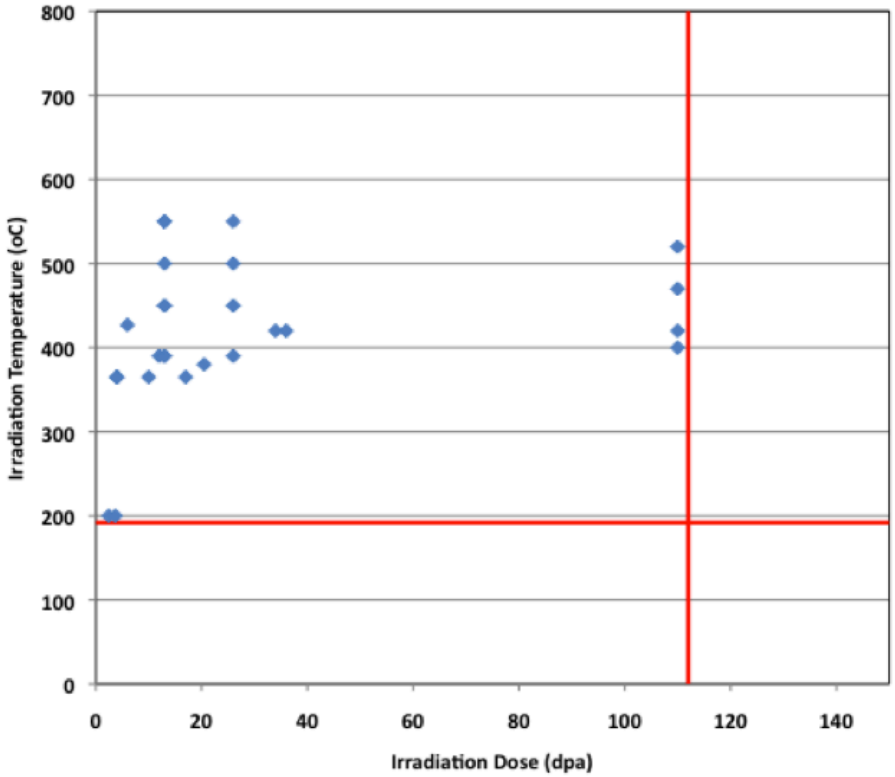

Fig. 20: Matrix of experimental data available on HT-9 DBTT shifts. Red lines indicate doses larger than 110 dpa and irradiation temperatures below 200°C.

Computer simulation and modeling of FeCr based materials under irradiation could help further the understanding of microstructural effects in F/M steels. DBTT shift after irradiation is attributed to matrix hardening as a result of alpha-prime formation, carbide precipitation, dislocation loop formation, etc. USE reduction is also attributed to changes in the microstructure (carbide precipitation and intermetallic formation, etc.). Understanding materials response under irradiation at the atomistic level is crucial to the development of radiation-resistant materials for future advanced fission reactors and fusion designs [44]. Prediction of how these materials will perform under high exposures represents a challenge to the capabilities of present day available models. Recently, Cr-cluster formation mechanisms under irradiation have been investigated via Molecular Dynamics simulations using an approach that takes advantage of empirical interatomic potentials developed based thermodynamic properties of the Fe-Cr system, experimental data and ab-initio results [45]. Multiscale modeling will be required to give insight into the derivation of physically based F/M steels embrittlement trendlines.

References

[1] S. A. Maloy, M. Toloczko, J. Cole, T. S. Byun, "Core materials development for the fuel cycle R&D program", J. of Nucl. Mater. 415 (2011) 302-305.

[2] T.R. Allen, J.T. Busby, R. L. Klueh, S. A. Maloy, M.B. Toloczko, "Cladding and duct materials for advanced nuclear recycle reactors", J. of the Minerals, Metals and Materials Society JOM 60 (2008) 15-23.

[3] R.L. Klueh and D.R. Harries, "High-Chromium Ferritic and Martensitic Steels for Nuclear Applications", American Society for Testing and Materials, ASTM Stock Number: MONO3, ASTM, West Conshohocken, PA 19428-2959.

[4] Standard Methods for Notched Bar Impact Testing of Metallic Materials, ASTM-E 23-82, Annual Book of ASTM Standards Volume 03.01 developed by Subcommittee E28.07 (West Conshohocken, PA) p. 277-299, 1982.

[5] G. E. Lucas and D.S. Gelles, "The influence of irradiation on fracture and impact properties of fusion reactor materials", J. of Nucl. Mater 155-157 (1988) 164-177.

[6] G.R. Odette and G.E. Lucas, "Embrittlement of nuclear reactor pressure vessels", J. of the Minerals, Metals, JOM 53 (7) (2001) 18-22.

[7] C.Z. Serpan, Jr. and L.E. Steele, "Damaging neutron exposure criteria for evaluating the embrittlement of reactor pressure vessel steels in different neutron spectra", Naval Research Laboratory NRL Report 6415 (1966).

[8] S.I. Porollo, A.M. Dvoriashin, Y.V. Konobeev, F.A. Garner, "Structure and mechanical properties of ferritic/martensitic steel EP-823 after neutron irradiation to high doses in BOR-60", J. of Nucl. Mater. 329 (2004) 314-318.

[9] J. S. Cheon, C.B. Lee, B.O. Lee, J. P. Raison, T. Mizuno, F. Delage, J. Carmack, "Sodium fast reactor evaluation: Core materials", J. of Nucl. Mater. 392 (2009) 324-330.

[10] S.N. Rosenwasser, P. Miller, J.A. Dalessandro, J.M. Rawls, W.E. Toffolo and W. Chen, J. of Nucl. Mater. 85&86 (1979) 177-182.

[11] G. R. Odette, "On the ductile to brittle transition in martensitic stainless steels – Mechanisms, models and structural implications", J. of Nucl. Mater. 212-215 (1994) 45-51.

[12] R.L. Klueh, A. T. Nelson, "Ferritic/martensitic steels for next-generation

reactors", J. of Nucl. Mater. 371 (2007) 37-52.

[13] E. A. Little, D. R. Harries, F. B. Pickering, and S. R. Keown, "Effects of Heat Treatment on Structure and Properties of 12%Cr Steel"', Metals Technology, Vol. 4, 1977, pp. 20-217.

[14] D. S. Gelles, “Swelling in several commercial alloys irradiated to very high neutron fluence”, J. of Nucl. Mater. 122 & 123 (1984) 207-213.

[15] D.S. Gelles, “Microstructural examination of commercial ferritic alloys at 200 dpa”, J. of Nucl. Mater. 233 (1996) 293-298.

[16] D. S. Gelles, “Development of martensitic steels for high neutron damage applications”, J. of Nucl. Mater. 239 (1996) 99-106.

[17] T.J. Trapp, P. Peterson, P. McClure, R. Kapernick, D. Poston, “Hyperion Power Module, Safety and Operational Features for Reactor Operations”, Transactions of the American Nuclear Society TANSAO 102 (2010) 365-366.

[18] J. Zhang, R.J. Kapernick, P.R. McClure, “Lead-bismuth Eutectic Technology for HYPERION”, Transactions of the American Nuclear Society TANSAO 102 (2010) 810-811.

[19] R.L. Klueh, D. J. Alexander, "Heat treatment effects on impact toughness of 9Cr–1MoVNb and 12Cr–1MoVW steels irradiated to 100 dpa", J. of Nucl. Mater. 258-263 (1998) 1269-1274.

[20] F.H. Huang, D.S. Gelles, "Impact Fracture Behavior of HT9 Duct", WHC-SA-2512-FP, Prepared for the U.S. DOE, Office of Env. Rest. and Waste Management, Westinghouse Hanford Company, Richland, Washington (July 1994).

[21] W-L Hu, D. S. Gelles, “The Ductile-to-Brittle Transition Behavior of Martensitic Steels Neutron Irradiated to 26 dpa”, Influence of Radiation on Material Properties, 13th International Symposium (Part II), ASTM STP 956, F. A. Garner, C. H. Henager, Jr. and N. Igata, Eds. American Society for Testing and Materials, Philadelphia, 1987, pp 83-97.

[22]R. J. Puigh, and N.F. Panayotou, "Specimen preparation and loading for the AD-2 Ferritic Experiment", ADIP Quarterly Progress Report, DOE/ER-0045/3, 30 June 1981, pp 261-293.

[23] A. M. Ermi, "Summary of the EBR-II AD-2 Ferritics Irradiation Experiment", HEDL--7461/DE89-010141, Westinghouse Handford Company report prepared for DOE June 1984.

[24] Ermi, A. M., "Reconstitution of the AD-2 Ferritic Experiment", ADIP Semiannual Progress Report DOE/ER-0045/8, 31 March 1982, pp. 431-444.

[25] G.R. Odette, P.M. Lombrozo, J.F. Perrin, and R.A. Wullaert, “Physically Based Regression Correlations of Embrittlement Data From Reactor Pressure Vessel Surveillance Programs”, EPRI NP-3319, Electric Power Research Institute, 1984.

[26] T. Lechtenberg, “Irradiation Effects in Ferritic Steels”, J. of Nuclear Materials 133&134 (1985) 149-155.

[27] W.L. Hu, “Miniature Charpy Impact Test Results for Irradiated Ferritic Alloys”, in Alloy Development for Irradiation Performance DOE/ER-0045/9, Semiannual Progress Report (September 30, 1982), p 255-271.

[28] W.R. Corwin, J. M. Vitek and R. L. Klueh, "Effect of Nickel Content of 9Cr-1MoVNb and 12Cr-1MoVW steels on the aging and irradiation response of impact properties", J. of Nucl. Mater. 149 (1987) 312-320.

[29] W.R. Corwin, R.L. Klueh and J.M. Vitek, “Effect of specimen size and nickel content on the impact properties of 12Cr-1MoVW ferritic steel”, J. Nucl. Mater. 122 & 123 (1984) 343 - 348.

[30] L. Seran, A. Alamo, A. Maillard, H. Touron, J. C. Brachet, P. Dubuisson, O. Rabouille, "Pre- and post-irradiation mechanical properties of ferritic-martensitic steels for fusion applications: EM10 base metal and EM10/EM10 welds", J. of Nucl. Mater. 212-215 (1994) 588-593.

[31] P. Dubuisson, D. Gilbon and J.L. Seran, “Microstructural evolution of ferritic-martensitic steels irradiated in the fast breeder reactor Phenix”, J. Nucl. Mater. 205 (1993) 178-189.

[32] R.L. Klueh, D. J. Alexander, “Impact behavior of 9Cr-1MoVNb and 12Cr-1MoVW steels irradiated in HFIR”, J. of Nucl. Mater. 179-181 (1991) 733-736.

[33] J. M. Vitek, W. R. Corwin, R. L. Klueh, J. R. Hawthorne, “On the saturation of the DBTT shift of irradiated 12Cr-1MoVW with increasing fluence”, J. of Nucl. Mater. 141-143 (1986) 948.

[34] R. L. Klueh and D. J. Alexander, “Irradiation Effects on Impact Behavior of 12Cr-1MoVW and 21/4Cr-1Mo Steels”, in :Effects of Radiation on Materials: 15th International Symp. ASTM STP 1125, Eds. R. E. Stoller, A. S. Kumar, and D. S. Gelles (American Society for Testing and Materials, Philadelphia 1992) 1256-1266.

[35] Small Specimen Test Techniques, 4th Volume ASTM STP 1418, Editors: M. Sokolov, J. D. Landes, G. E. Lucas, ASTM International Committee E10 on Nuclear Technology and Applications, Aug 1, 2002 - 494 pages.

[36] J. R. Hawthorne and F.A. Smidt, Jr., “Evaluation of fracture resistance of ferritic stainless steels for first wall and blanket applications”, J. of Nucl. Mater. 103 & 104 (1981) 883-886.

[37] R.L. Klueh and D. J. Alexander, “Heat treatment effects on toughness of 9Cr-1MoVNb and 12Cr-1MoVW steels irradiated at 365°C”, J. of Nucl. Mater. 191-194 (1992) 896-900.

[38] R. L. Klueh and D. J. Alexander, “Charpy Impact Toughness of Martensitic Steels Irradiated in FFTF: Effect of Heat Treatment”, Effects of Radiation on Materials: 16th International Symposium, ASTM STP 1175, Eds., American Society for Testing and Materials, Philadelphia, 1993.

[39] E. Lucon and A. Almazouzi, “Irradiation behaviour of three candidate structural materials for ADS systems: EM10, T-91, and HT-9 (F/M Steels)”,SCK•CEN, Mol, Belgium, EUROMAT 2005 –Prague, Czech Republic, Sep 5-8, 2005.

[40] A. Almazouzi, E. Lucon, “Mechanical behavior of neutron irradiated high Cr ferritic-martensitic steels”, TMS Letters 2, 3 (2005) 73-74.

[41] H. Ait Abderrahim, Th. Aoust, E. Malambu, V. Sobolev, K. Van Tichelen, D. De Bruyn, D. Maes, W. Haeck and G. Van den Eynde, “MYRRHA, A Pb-Bi Experimental ADS: Specific approach to radiation protection aspects”, Rad. Prot. Dos. 116 (2005) 433-441. http://myrrha.sckcen.be/].

[42] T. S. Byun, W. D. Lewis, M. B. Toloczko, S. Maloy, “Impact properties of irradiated HT9 form the fuel duct of FFTF”, J. Nucl. Mater. 421 (2012) 104-111.

[43] S. A. Maloy, "Clad and Duct Materials Property Needs for Sodium Fast Reactors: US Perspective", Int. Fast Reactor Working Group, Tokyo, Japan, May 15h, 2009. LA-UR-09-02118.

[44] G. R. Odette and G. E. Lucas, “Embrittlement of nuclear reactor pressure vessels”, Journal of the Minerals, Metals and Materials Society, JOM July 2001, 18-22.

[45] A. Caro, J. Hetherly, A. Stukowski, M. Caro, E. Martinez, S. Srivilliputhur, L. Zepeda-Ruiz, M. Nastasi, “Properties of Helium bubbles in Fe and FeCr alloys”, J. of Nucl. Mater. 418 (2011) 261.

ANNEX

In Table I, composition limits are given for austenitic stainless steels tubing; taken from the guideline ASTM 771/A 771 M -95 (2001). 316 SS conforms to TP316, D-9 conforms to S38660 (D-9 is a Ti modified variant of 316 SS) and HT-9 conforms to UNS S42100.

Table I: Alloy composition Limits for Austenitic Stainless Steel Tubing.

Element	**TP 316 S31600**	**S38660**	**S42100**
Carbon	0.040-0.060	0.030-0.050	0.17-0.23
Manganese	1.00-2.00	1.65-2.35	0.40-0.70
Phosporous, max	0.040	0.040	0.040
Sulfur, max	0.010	0.010	0.010
Silicon	0.50-0.75	0.50-1.00	0.20-0.30
Nickel	13.0-14.0	14.5-16.5	0.30-0.80
Chromium	17.0-18.0	12.5-14.5	11.0-12.5
Molybdenum	2.00-3.00	1.50-2.50	0.80-1.20
Titanium	---	0.10-0.40[A]	---
Columbium, max	0.050	0.050	0.050 max
Tantalum, max	0.020	0.020	---
Tungsten	---	---	0.40-0.60
Nitrogen, max	0.010	0.005	---
Aluminun, max	0.050	0.050	0.050
Arsenic, max	0.030	0.030	---
Boron, max	0.0020	0.0020	---
Cobalt, max	0.050	0.050	---
Copper, max	0.04	0.04	---
Vanadium, max	0.05	0.05	0.25-0.35

[A]: Aim for 0.25

Columbium: Niobium (Nb)